

**Optimal hot metal desulphurisation slag considering iron loss and sulphur removal capacity part II evaluation**

Schrama, Frank N.H.; Beunder, Elisabeth M.; Panda, Sourav K.; Visser, Hessel Jan; Moosavi-Khoonsari, Elmira; Hunt, Adam; Sietsma, Jilt; Boom, Rob; Yang, Yongxiang

**DOI**

[10.1080/03019233.2021.1882648](https://doi.org/10.1080/03019233.2021.1882648)

**Publication date**

2021

**Document Version**

Final published version

**Published in**

Ironmaking and Steelmaking

**Citation (APA)**

Schrama, F. N. H., Beunder, E. M., Panda, S. K., Visser, H. J., Moosavi-Khoonsari, E., Hunt, A., Sietsma, J., Boom, R., & Yang, Y. (2021). Optimal hot metal desulphurisation slag considering iron loss and sulphur removal capacity part II: evaluation. *Ironmaking and Steelmaking*, 48(1), 14-24. <https://doi.org/10.1080/03019233.2021.1882648>

**Important note**

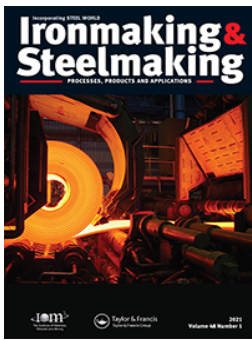
To cite this publication, please use the final published version (if applicable). Please check the document version above.

**Copyright**

Other than for strictly personal use, it is not permitted to download, forward or distribute the text or part of it, without the consent of the author(s) and/or copyright holder(s), unless the work is under an open content license such as Creative Commons.

**Takedown policy**

Please contact us and provide details if you believe this document breaches copyrights. We will remove access to the work immediately and investigate your claim.



# Ironmaking & Steelmaking

Processes, Products and Applications

ISSN: (Print) (Online) Journal homepage: <https://www.tandfonline.com/loi/yirs20>

## Optimal hot metal desulphurisation slag considering iron loss and sulphur removal capacity part II: evaluation

Frank N. H. Schrama, Elisabeth M. Beunder, Sourav K. Panda, Hessel-Jan Visser, Elmira Moosavi-Khoonsari, Adam Hunt, Jilt Sietsma, Rob Boom & Yongxiang Yang

To cite this article: Frank N. H. Schrama, Elisabeth M. Beunder, Sourav K. Panda, Hessel-Jan Visser, Elmira Moosavi-Khoonsari, Adam Hunt, Jilt Sietsma, Rob Boom & Yongxiang Yang (2021) Optimal hot metal desulphurisation slag considering iron loss and sulphur removal capacity part II: evaluation, *Ironmaking & Steelmaking*, 48:1, 14-24, DOI: [10.1080/03019233.2021.1882648](https://doi.org/10.1080/03019233.2021.1882648)

To link to this article: <https://doi.org/10.1080/03019233.2021.1882648>



© 2021 The Author(s). Published by Informa UK Limited, trading as Taylor & Francis Group



Published online: 04 Mar 2021.



[Submit your article to this journal](#)



Article views: 300



[View related articles](#)



[View Crossmark data](#)

## Optimal hot metal desulphurisation slag considering iron loss and sulphur removal capacity part II: evaluation

Frank N. H. Schrama <sup>a,b</sup>, Elisabeth M. Beunder <sup>b</sup>, Sourav K. Panda <sup>b</sup>, Hessel-Jan Visser <sup>b</sup>, Elmira Moosavi-Khoonsari <sup>b,\*</sup>, Adam Hunt <sup>c</sup>, Jilt Sietsma <sup>a</sup>, Rob Boom <sup>a</sup> and Yongxiang Yang <sup>a</sup>

<sup>a</sup>Department of Materials Science and Engineering, Delft University of Technology, Delft, Netherlands; <sup>b</sup>Tata Steel, IJmuiden, Netherlands;

<sup>c</sup>Materials Processing Institute, Middlesbrough, UK

### ABSTRACT

The optimal hot metal desulphurisation (HMD) slag is defined as a slag with a sufficient sulphur removal capacity and a low apparent viscosity ( $\eta_{slag}$ ) which leads to low iron losses. In part I of this study, the fundamentals behind the optimal slag were discussed. In this part these fundamentals are explored by a Monte Carlo simulation, based on FactSage calculations, plant data analysis and melting point and viscosity measurements of the optimal slag. Furthermore, the applicability of knowing the optimal slag composition for an industrial HMD is discussed.

Abbreviations: BF: Blast furnace; HMD: Hot metal desulphurisation; MCS: Monte Carlo simulation; RFM: Random forest model; XRF: X-ray fluorescence

### ARTICLE HISTORY

Received 27 November 2020  
Revised 18 January 2021  
Accepted 20 January 2021

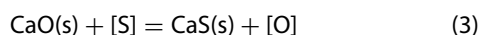
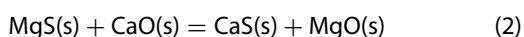
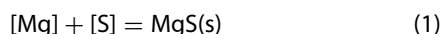
### KEYWORDS

Hot metal desulphurisation; slag; iron loss; sulphide capacity; thermodynamics; Monte Carlo simulation; industrial data; viscosity and melting point experiments

## Introduction

Slag is an important aspect of the hot metal desulphurisation (HMD) process, as it has to contain the sulphur that is removed from the hot metal by the reagents magnesium and lime. The slag also leads to iron losses in the HMD process, both by entrapping iron droplets ('colloid loss') and by entraining iron when the slag is skimmed off ('entrainment loss'). The aim of this study is to find the composition of the optimal slag for the magnesium-lime co-injection HMD process for sulphur removal as well as iron losses. In part I of this study [1], the influence of slag composition on its sulphur removal capacity and on the iron loss was described. In part II, which is presented in this paper, the theory from part I is evaluated with a Monte Carlo simulation (MCS) using thermodynamic modelling data from FactSage 7.3 [2], with viscosity and melting point measurements of the optimal slag and with industrial data from the Tata Steel plant in IJmuiden, the Netherlands.

As for the magnesium-lime co-injection HMD process, the main desulphurisation reactions (reactions 1–2) take place in the hot metal, after which the sulphur is stabilised in the slag [3–5].



Therefore, the slag and hot metal are not in equilibrium with regards to sulphur distribution, which was validated with plant data [1]. This means that an HMD slag with a sufficient sulphur removal capacity should contain enough

lime to react with sulphur (reactions 2 and 3) and should have a high enough basicity to allow reaction 2 to proceed. Under industrial circumstances this is a  $B2 > 1.1$  [6]. The definition of  $B2$  (basicity) is given by the following equation:

$$B2 = \frac{X_{\text{CaO}}}{X_{\text{SiO}_2}} \quad (4)$$

Here  $X_{\text{CaO}}$  and  $X_{\text{SiO}_2}$  are the mass fractions of CaO and SiO<sub>2</sub>, respectively. The basicity of the HMD slag should at the same time be low to minimise the iron losses, because a higher  $B2$  leads to a higher solid fraction in the slag. Roughly half of the iron losses in an industrial HMD plant are caused by colloid losses (iron droplets captured in the slag in a colloid, which are removed together with the slag during skimming). These colloid losses can be reduced by decreasing the slag viscosity ( $\eta_{slag}$ ; in Pa·s). This  $\eta_{slag}$  depends on the viscosity of the liquid fraction of the slag ( $\eta_0$ ) and the slag's solid volume fraction ( $\varphi_{s,slag}$ ). The Einstein-Roscoe equation shows their dependence [7]:

$$\eta_{slag} = \eta_0 \cdot (1 - \varphi_{s,slag} \cdot \alpha)^{-n} \quad (5)$$

Here  $\alpha$  and  $n$  are empirical constants [1].

As was discussed in part I, different slag components have their influence on the sulphide capacity ( $C_S$ ), and thus the sulphur removal capacity, and on  $\eta_{slag}$ , either by changing the slag's solid fraction ( $X_{solid}$ ) or via  $\eta_0$ . Table 1 summarises the effect of the separate slag components, as well as the temperature, on  $C_S$ ,  $X_{solid}$  and  $\eta_0$ . It shows that slag components that lead to a higher  $C_S$ , thus a better sulphur removal capacity, often also lead to a higher  $\eta_{slag}$ , which results in higher iron losses. The optimal slag should find

**CONTACT** Frank N. H. Schrama  frank.schrama@tatasteleurope.com  Department of Materials Science and Engineering, Delft University of Technology, Mekelweg 2, 2628 CD, Delft, Netherlands; Tata Steel, PO Box 10000, 1970, IJmuiden, CA, Netherlands

\*Elmira Moosavi-Khoonsari now works with Aurubis, Hamburg AG, Germany

© 2021 The Author(s). Published by Informa UK Limited, trading as Taylor & Francis Group

This is an Open Access article distributed under the terms of the Creative Commons Attribution-NonCommercial-NoDerivatives License (<http://creativecommons.org/licenses/by-nc-nd/4.0/>), which permits non-commercial re-use, distribution, and reproduction in any medium, provided the original work is properly cited, and is not altered, transformed, or built upon in any way.

**Table 1.** Effect of separate slag components and temperature on  $C_s$ ,  $T_{liq}$  and  $\eta_0$ , impact is indicated ranging from ▼▼ (very negative) to ▲▲ (very positive) [1].

Component	$C_s$	$X_{solid}$	$\eta_0$
CaO	▲▲	▲▲	▼
SiO <sub>2</sub>	▼	▼	▲
Al <sub>2</sub> O <sub>3</sub>	▼	▼	▲
MgO	0	▲▲	▼
TiO <sub>2</sub>	▼	▼	▼
Na <sub>2</sub> O	▲	▼	▼
K <sub>2</sub> O	▲	▼	▼
MnO	▲	▼	▼
CaF <sub>2</sub>	▼	▼▼	▼
CaCl <sub>2</sub>	0	▼	▼
FeO <sub>n</sub>	▼	▼	▼
Temperature	▲	▼	▼

the balance between a high sulphur removal capacity and low iron losses.

## HMD slag thermodynamic simulation

### Monte Carlo simulation input

To get a better picture of the thermodynamic influence of all slag components on the solid weight fraction ( $X_{solid}$ ), a Monte Carlo simulation (MCS) was done with FactSage 7.3 [2] (using CON2, a consortium database), with 18,776 different HMD slag compositions. In this MCS, realistic values are used for the slag composition and its temperature, but, unlike industrial slags, these values have no interdependences. Within the given ranges, the slag composition of the MCS is completely random. With industrial slags, the concentration of several components is correlated, because they are influenced in the same way by the BF process, or because BF operation actively aims for certain composition ratios (for example B2). Therefore, the MCS allows analysis of the influence of individual components on  $C_s$  and iron loss, which is not possible with analysis of industrial data. Table 2 gives the ranges that were used for the MCS.

It should be noted that the total composition is always normalised to 100%, which leads to a skewed distribution of the weight fractions of, especially, CaO, Al<sub>2</sub>O<sub>3</sub>, SiO<sub>2</sub> and MgO. Higher weight fractions appear to be less frequent.

### Solid fraction

For optimal HMD slag, the solid fraction ( $X_{solid}$ ) should be low. To analyse which components, thermodynamically, lead to a low solid fraction, a random forest model (RFM) is created based on the MCS data. This RFM is based on 50 decision trees, each with an end node size of at least 10. With this

**Table 2.** Composition and temperature ranges of the slags in the MCS.

Component	Min (wt-%)	Max (wt-%)
CaO	25	50
Al <sub>2</sub> O <sub>3</sub>	0	20
SiO <sub>2</sub>	10	40
MgO	5	30
MnO	0	5
FeO	0	10
TiO <sub>2</sub>	0	5
P <sub>2</sub> O <sub>5</sub>	0	3
V <sub>2</sub> O <sub>5</sub>	0	3
Cr <sub>2</sub> O <sub>3</sub>	0	3
Na <sub>2</sub> O	0	5
K <sub>2</sub> O	0	5
Temperature	1150°C	1500°C

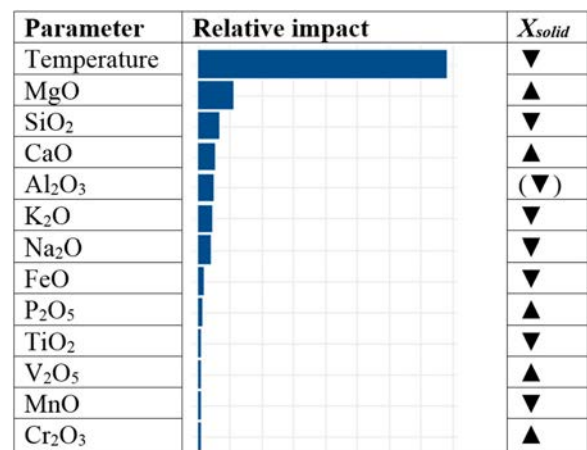
model, it is determined how well the output,  $X_{solid}$ , can be predicted based on the parameters, in this case the slag components and temperature. Figure 1 shows the impact, relative to the distribution, of the parameter on  $X_{solid}$ , and whether an increase in this parameter leads to an increase (▲) or decrease (▼) of  $X_{solid}$ . The larger the impact, the more  $X_{solid}$  can be influenced by changing that parameter.

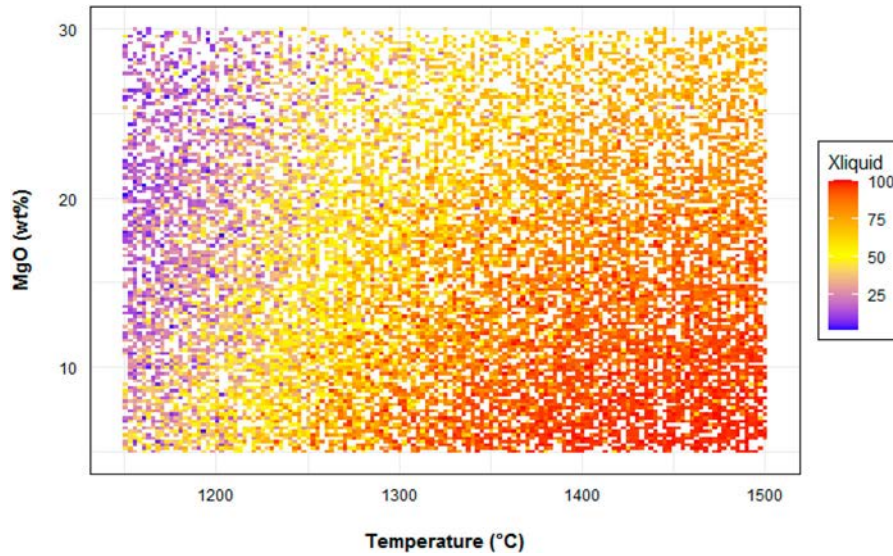
The RFM shows that temperature has the largest influence on  $X_{solid}$ , which is in agreement with literature. Because CaO, SiO<sub>2</sub>, Al<sub>2</sub>O<sub>3</sub> and MgO have the largest fractions in the HMD slag, also in the MCS, their influence on  $X_{solid}$  is the most significant as well. Here MgO and, to lesser extent, CaO increase  $X_{solid}$ , while SiO<sub>2</sub> decreases  $X_{solid}$ . Al<sub>2</sub>O<sub>3</sub> decreases  $X_{solid}$  as well, but above 12 wt-% it starts to increase  $X_{solid}$ . This is all in accordance with the theory, as discussed in part I [1]. It is remarkable that the relative impact of alkali metal oxides, K<sub>2</sub>O and Na<sub>2</sub>O, on  $X_{solid}$  is in the same order of magnitude as the impact of CaO and Al<sub>2</sub>O<sub>3</sub>. Alkali metal oxides are known to have a strong effect on  $T_{melt}$  of a slag [8]. Furthermore, FeO only has a small impact on lowering  $X_{solid}$  according to the MCS. This is remarkable, as in part I it was explained, based on FactSage calculations, that FeO lowers  $T_{liq}$ , and thus  $X_{solid}$ . However, because the MCS was done under inert conditions, so no free oxygen, FeO itself does not shift between the solid and liquid phase. FeO does lower  $T_{melt}$ , but this only influences  $X_{solid}$  of the slag if the temperature of the slag is close to this  $T_{melt}$ . As the temperature in the MCS ranges from 1150 to 1500°C, this is only the case for a small portion of the simulated slags, hence the small impact of FeO on  $X_{solid}$  in the MCS. The impact of the remaining minor elements is low, as could be expected.

Figure 2 gives a heat map of the influence of the two most important parameters, temperature and MgO, on  $X_{solid}$  (in the heat map  $X_{liquid}$  is depicted), based on the MCS results. It indicates that when the MgO concentration in the slag is decreased by 1 weight per cent point, the slag temperature can be roughly 4°C lower to have the same  $X_{solid}$ , and thus the same iron losses.

### Sulphur removal capacity

As this MCS assumes a homogeneous slag at equilibrium, the sulphide capacity ( $C_s$ ) is used to determine the sulphur

**Figure 1.** Relative impact, corrected for the distribution, of the parameters of the MCS on  $X_{solid}$ , according to the random forest model. The right column shows if  $X_{solid}$  is increased (▲) or decreased (▼) by increase in the parameter value.



**Figure 2.** Heat map of  $X_{liquid}$  as a function of temperature (x-axis) and MgO concentration (y-axis).

removal capacity of the slag, as is explained in part I [1].  $C_S$  is calculated with Equation (6):

$$C_S = X_{(S)} \sqrt{\frac{p_{O_2}}{p_{S_2}}} \quad (6)$$

Here  $X_{(S)}$  is the weight percentage of all sulphides in the slag and  $p_{O_2}$  and  $p_{S_2}$  are the partial pressures for oxygen and sulphur, respectively. The calculations were performed at a fixed  $p_{O_2} = 10^{-6}$  atm. and  $p_{S_2} = 10^{-4}$  atm [1]. The current calculations do not take into consideration the effect of  $p_{O_2}$  and  $p_{S_2}$  on  $C_S$ , which plays a part in high sulphides containing slag

(~ 10wt.% CaS in HMD slag). The role of  $p_{O_2}$  and  $p_{S_2}$  for  $C_S$  calculations is explained by Moosavi-Khoonsari and Jung [9]. To see the thermodynamic influence of the independent slag components on  $C_S$ , a density plot is made based on the MCS results, showing the slags with the highest 25%  $C_S$  and with the highest 25%  $X_{liquid}$  (see Figure 3). The density plot visualises the influence of an individual slag component on  $C_S$ .

The difficulty in designing an optimal HMD slag is well illustrated by a comparison of the MCS results for  $X_{liquid}$  and the results for  $C_S$ . Oxides that are thermodynamically beneficial for a high  $X_{liquid}$  (and thus a low  $X_{solid}$ ), like  $SiO_2$ , also lead to a low  $C_S$ . CaO increases the  $C_S$ , but decreases

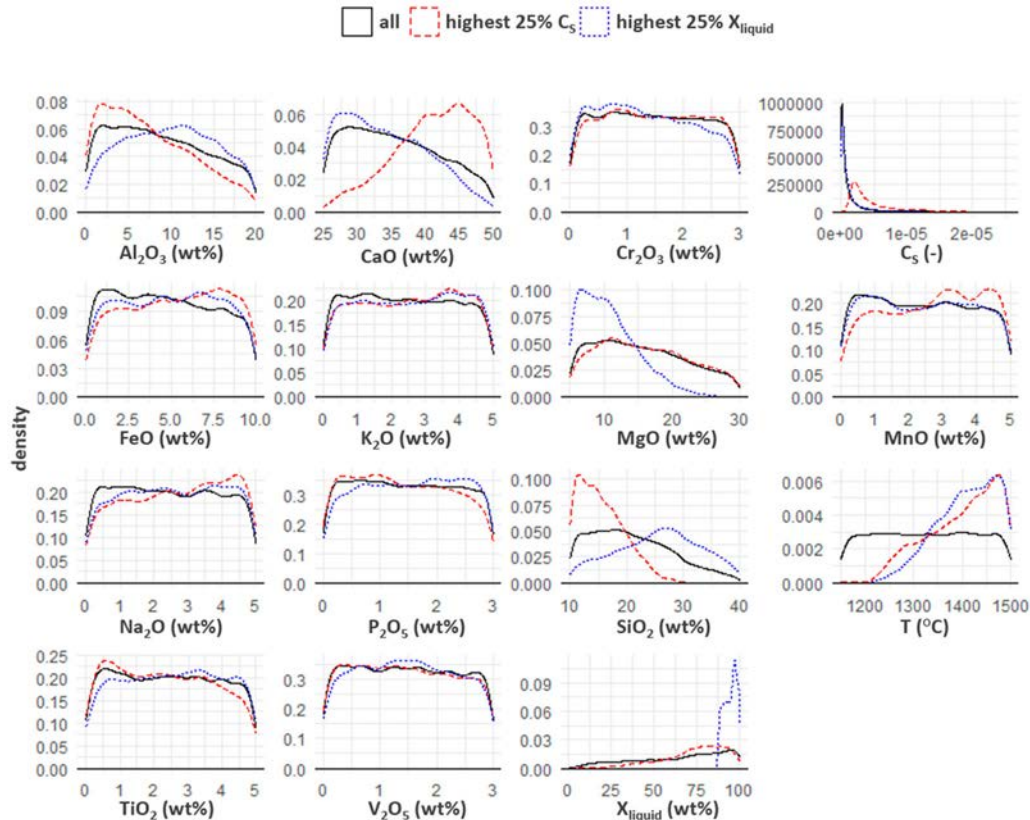


**Figure 3.** Density plot of the slag components, temperature,  $C_S$  and  $X_{liquid}$  for the complete dataset (solid black line), the 25% slags with the highest  $C_S$  value (dashed red line) and the 25% slags with the highest  $X_{liquid}$  from the MCS.



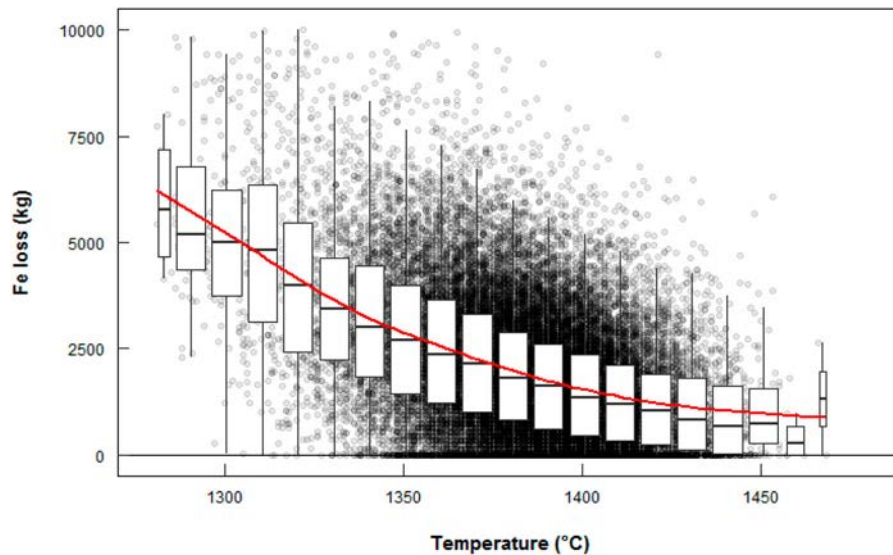


**Figure 5.** Iron loss (in kg) at different hot metal temperatures at the HMD stations of Tata Steel in IJmuiden, the Netherlands. Boxes stretch from the 25th till the 75th percentile of the distribution. The lines (whiskers) extend to 1.5 times the interquartile range. The trendline is polynomial. The circles represent individual heats.

(together as  $B2$ ),  $Al_2O_3$  and  $MgO$ . The  $SiO_2$  and  $Al_2O_3$  concentration depend on the BF carryover slag composition only, which is quite constant during stable BF operation. For this study, an average BF carryover slag composition is used. Therefore, the effect of  $Al_2O_3$  and  $SiO_2$  cannot be studied on a heat basis. As the amount of injected  $CaO$  and  $Mg$  (which ends up as  $MgO$  in the slag, see reaction 2) are known, their effect on the iron losses can be analysed with plant data (see Figure 7).

Figure 7 shows the iron concentration in skimmed off slag, calculated by dividing total iron loss by total skimmed off slag weight, at different  $B2$  values. The influence of  $B2$  can be analysed independent of the total slag weight. As is expected, based on the thermodynamics [1], a higher  $B2$ , which means more  $CaO$ , leads to higher iron losses. However, below a  $B2$  of 1.7 there seems to be no correlation between basicity and iron losses. As explained in part I,  $B2$  influences  $\eta_{slag}$  mostly by influencing the solid fraction, as a higher  $B2$  leads to a higher  $T_{melt}$  under HMD conditions. Possibly, at the typical HMD temperatures (mean hot metal temperature

in this data set is  $1390^\circ C$ ) the slag has a liquid fraction  $>90$  wt-% at  $B2 < 1.7$ . This would mean that lowering the  $B2$  would hardly influence  $\eta_{slag}$ . The thermodynamic calculations in part I indicate that a lower  $B2$  is required to reach a liquid slag, but in that calculation the influence of minor slag elements, like  $FeO_x$  or alkali metal oxides, which lower  $\eta_{slag}$ , was neglected.

Figure 8 shows the correlation between  $MgO$  fraction in the slag and iron losses. The plant data clearly show that for  $MgO$  concentrations above 14 wt-%, the iron losses increase. Although total slag weight increases with the  $MgO$  concentration in the slag, the slag weight has only little effect on the correlation between  $MgO$  concentration and iron losses. It is in line with the theory, that a higher  $MgO$  concentration in the slag leads to a higher solid fraction, and thus to a higher  $\eta_{slag}$ , which finally leads to higher iron losses [1]. It should be noted that for  $MgO$  concentrations below 14 wt-%, the iron losses do not further decrease, although that would be expected based on the theory. As at  $B2 < 1.7$   $\eta_{slag}$  is not affected significantly because the slag

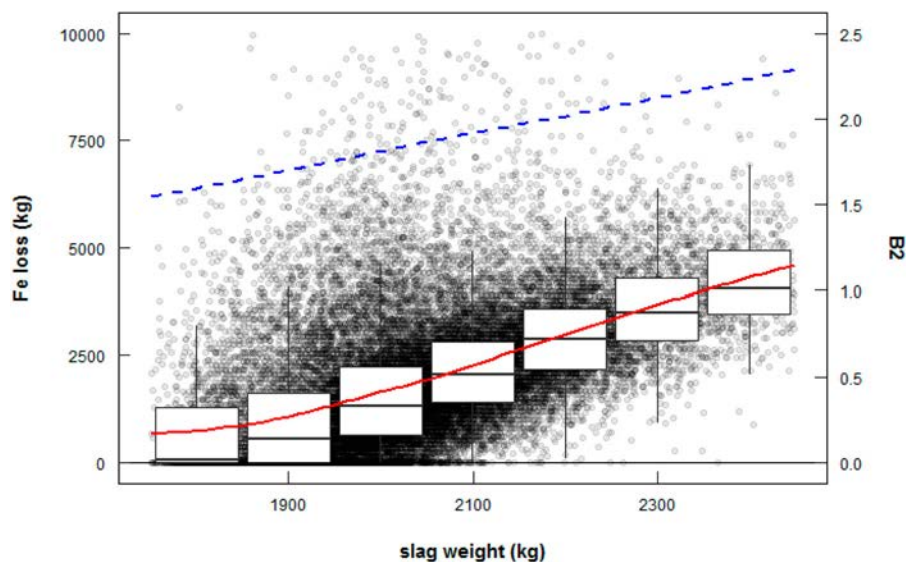


**Figure 6.** Iron loss (red solid line) and  $B2$  (blue dashed line) at different slag weights at the HMD stations of Tata Steel in IJmuiden, the Netherlands. Boxes stretch from the 25th till the 75th percentile of the distribution. The lines (whiskers) extend to 1.5 times the interquartile range. The circles represent individual heats.

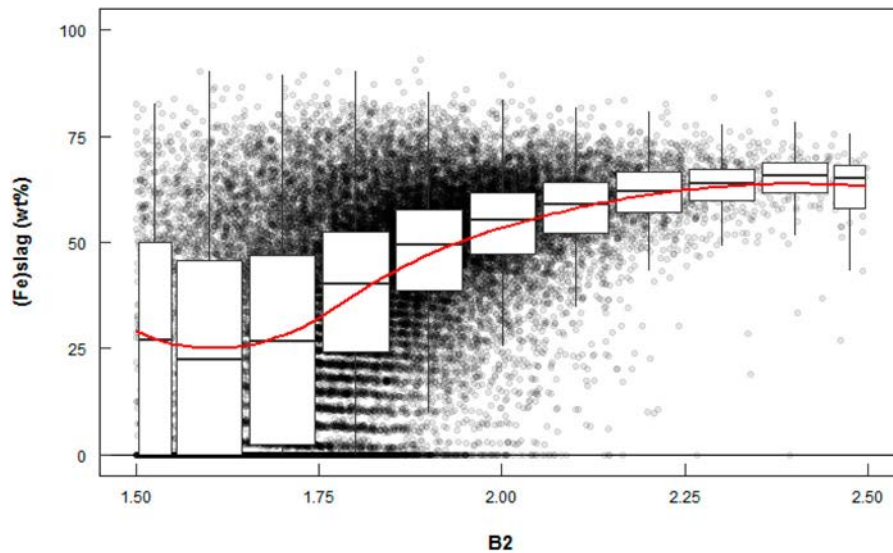


**Figure 7.** Iron concentration in skimmed off slag at different  $B2$  values at the HMD stations of Tata Steel in IJmuiden, the Netherlands. Boxes stretch from the 25th till the 75th percentile of the distribution. The lines (whiskers) extend to 1.5 times the interquartile range. The circles represent individual heats.

is already liquid, also  $MgO$  fractions below 14 wt-% probably do not lead to lower iron losses anymore, as the slag is liquid at  $MgO < 14$  wt-% under the HMD conditions in the data set.

### Silicon and titanium

$TiO_2$  is identified as a component that influences  $\eta_{slag}$ . However, in an industrial blast furnace,  $TiO_2$  is correlated with  $SiO_2$  in the slag, as are Ti and Si in the hot metal. This means that industrial slags with a high  $SiO_2$  concentration will be high in  $TiO_2$  as well [12]. Therefore, it is not possible to identify an independent correlation between  $TiO_2$  in the slag and iron losses with this plant data analysis.

To understand the effect of silicon concentration in the hot metal on iron losses, independent from  $B2$ , the correlation between silicon in hot metal and iron losses is investigated. Besides the correlation between silicon and titanium in hot metal, there is a strong reverse correlation between silicon and sulphur in the hot metal, which leads to a

correlation with the slag weight as higher sulphur removal requires more reagents being injected. In general, a higher oxygen activity,  $a_O$ , in the hot metal at the BF leads to less silicon in the hot metal and more  $SiO_2$  in the slag.  $SiO_2$  decreases the  $B2$ , so less desulphurisation takes place in the BF, leading to more sulphur in the hot metal [12,13]. The plant data confirm the correlation between silicon and sulphur at silicon levels  $< 0.5$  wt-%. However, for silicon concentration  $> 0.5$  wt-%, the reversed correlation between silicon in the metal and  $SiO_2$  in the slag becomes weaker. This is because high silicon concentrations ( $> 0.5$  wt-%) are typically caused by more silicon in the BF in total (Si in hot metal +  $SiO_2$  in slag). Therefore, at silicon levels  $> 0.5$  wt-%, the correlation between silicon in the hot metal and  $B2$ , and thus between silicon and sulphur in the hot metal, decreases.

Figure 9 shows the correlation between silicon in the hot metal and the iron losses (solid red line). For  $[Si] < 0.5$  wt-%, an increasing silicon fraction correlates with a decreasing

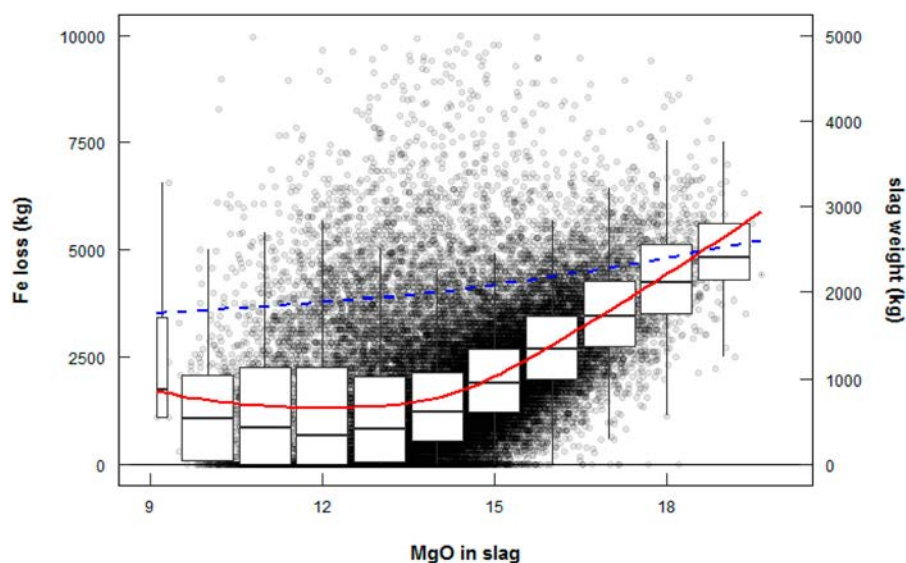


**Figure 8.** Iron loss (red solid line) and slag weight (blue dashed line) at different  $MgO$  concentrations in the slag at the HMD stations of Tata Steel in IJmuiden, the Netherlands. Boxes stretch from the 25th till the 75th percentile of the distribution. The lines (whiskers) extend to 1.5 times the interquartile range. The circles represent individual heats.

sulphur concentration, thus with less reagents being injected, which ultimately leads to lower iron losses. For  $[\text{Si}] > 0.5$  wt-%, this phenomenon no longer dictates the iron losses, as the iron losses are now increasing with an increasing silicon concentration. It should be noted that the highest silicon concentrations ( $>0.8$  wt-%) are often the result of starting up the BF, when higher slag amounts, more sulphur and lower temperatures occur. However, there is an increase in iron losses at 0.5–0.7 wt-%  $[\text{Si}]$  as well, which cannot be explained by non-standard circumstances. The  $B_2$  of the slag (dashed blue line) does not change significantly at higher silicon concentrations, so it cannot explain the increasing iron losses. The increase cannot be explained by a different mean temperature, as high silicon concentrations correlate with higher hot metal temperatures [12,13], so a decrease in iron losses would be expected. One possible explanation is the titanium concentration, which correlates strongly with the silicon concentration in hot metal. A high titanium concentration in the hot metal will lead to a high  $\text{TiO}_2$  concentration in the slag and a high concentration of  $\text{Ti}(\text{C},\text{N})$  particles, which leads to a sticky, viscous slag [4,14]. Because the slag composition is not directly measured and the titanium and silicon in hot metal are too much correlated, this hypothesis cannot be proven with the current plant data. Another possible explanation is the  $a_{\text{O}}$ , as a low  $a_{\text{O}}$  in the BF hearth would lead to a higher silicon concentration in the hot metal. At a low  $a_{\text{O}}$ , it is expected that the  $\text{FeO}_x$  concentration in the slag will be low.  $\text{FeO}_x$  has a large influence on  $\eta_{\text{slag}}$ , so a slag with a low  $\text{FeO}_x$  concentration will have a high  $\eta_{\text{slag}}$  and, thus, high iron losses. As  $\text{FeO}_x$  and  $a_{\text{O}}$  are not measured, this hypothesis cannot be proven either with the current plant data.

## Discussion

Analysis of plant data identifies several factors that influence the iron losses during the HMD process. This analysis confirms the theory [1], that  $\eta_{\text{slag}}$  governs the iron losses, which is illustrated by the strong correlations of temperature,  $B_2$  and MgO concentration with the iron losses. It should be noted that both  $B_2$  and MgO increase when more CaO and Mg are

injected to desulphurise the hot metal. According to the theory, iron losses are also influenced by  $\text{TiO}_2$  and  $\text{FeO}_x$  concentration in the slag, as both oxides influence  $\eta_{\text{slag}}$ , but this cannot be confirmed by the plant data analysis.

The total slag weight also plays a role, albeit minor compared to MgO and  $B_2$ . Figure 7 shows that the basicity of the slag, and thus the  $\eta_{\text{slag}}$ , contributes more to the iron losses than the slag weight, which is correlated with  $B_2$ .

Although it was expected that less basic oxides in the slag would lead to a lower melting point, thus lower iron losses, there seems to be an optimal  $B_2$  and MgO concentration. Lowering the  $B_2$  below 1.7 or lowering MgO below 14 wt-% does not seem to significantly influence the iron losses. This is explained by the slag temperature. If a certain  $B_2$  or MgO concentration leads to a  $T_{\text{melt}}$  below the slag temperature, a further decrease in  $T_{\text{melt}}$  by changing the slag composition will not influence the iron losses. Therefore, the optimal  $B_2$  and MgO concentration in the slag depends on the slag temperature. It should be noted that for plants with an average hot metal temperature below  $1390^\circ\text{C}$ , the optimal  $B_2$  and MgO concentration will be lower.

## Viscosity and melting range experiments

### Introduction

To validate if optimal HMD slag, as described in this work, actually has a low apparent viscosity ( $\eta_{\text{slag}}$ ), experiments with a synthetic optimal HMD slag were done, where the viscosity and melting temperature were measured. The synthetic optimal HMD slags were prepared by mixing the necessary chemical components and prefusing them in a graphite crucible in a muffle furnace at  $1600^\circ\text{C}$  for 10 min. The prefused slags were then quenched on a steel plate and milled in a Tema mill for 30 s. The milled samples were decarburised at  $650^\circ\text{C}$  for 16 hr to remove any residual carbon that had been absorbed from the graphite crucible during prefusing. The composition of the tested slags is given in Table 3. The main difference between slag #1 and #2 is the  $\text{MgO}:\text{Al}_2\text{O}_3$  ratio. Slag #2 is considered the optimal

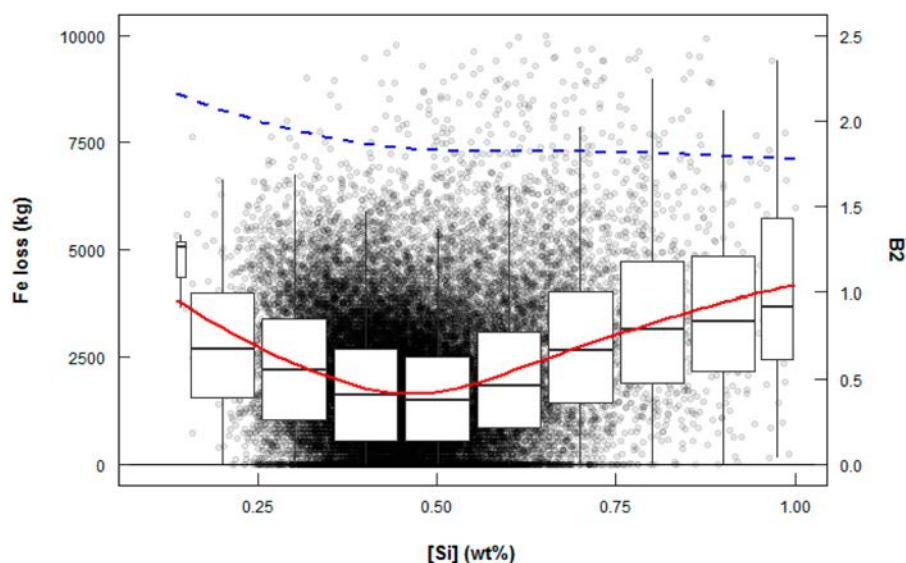


**Figure 9.** Iron losses (solid red line) and mean  $B_2$  (dashed blue line) at different silicon concentrations in hot metal,  $[\text{Si}]$  (in wt-%) at the HMD stations of Tata Steel in IJmuiden, the Netherlands. Boxes stretch from the 25th till the 75th percentile of the distribution. The lines (whiskers) extend to 1.5 times the interquartile range. The circles represent individual heats.

HMD slag, according to the theory, in terms of its main components CaO, SiO<sub>2</sub>, Al<sub>2</sub>O<sub>3</sub> and MgO.

It should be noted that the CaS value is low compared to industrial HMD slag, which typically contains around 13.5 wt-% CaS. When the synthetic slags were prepared, 13.5 wt-% of CaS was added to the slag. However, when the slag was heated to 1600°C to homogenise the slag components, the CaS reacted with oxygen to form CaO. The XRF analysis of the slags was done prior to the viscosity and melting point experiments.

For comparison, an industrial HMD slag sample and a synthetic HMD slag sample, both from a previous study by the authors [15], have been added to Table 3. Note that the industrial HMD sample contains a high amount of Fe<sub>2</sub>O<sub>3</sub>, which is mostly entrapped iron that oxidised during preparation for XRF analysis. During the melting point and viscosity measurements, part of the entrapped iron was already oxidised. The FeO<sub>x</sub> concentration in the slag during the HMD process is in the order of 1-3 wt-%. Slag 2.1 showed the closest resemblance to slag #1.

### Melting point measurements

For the melting point measurements, a Misura HM2-1600 heating microscope was used. Samples were prepared using a steel die to manually compress prefused powdered slag into cylinders of 3 mm in height and 2 mm in diameter. The samples were then placed onto an alumina plate and inserted into the horizontal tube furnace of the heating microscope. The samples were heated to 1100°C at 50° C min<sup>-1</sup> under inert conditions, after which they were heated to the melting point at 6°C min<sup>-1</sup>. The device is able to acquire and store images of the sample at 2°C intervals during the heating cycle. During the heating cycle, all the dimensional parameters of the sample were measured automatically in order to identify phase transitions of the material. The DIN 51730 standard was used to calculate  $T_{melt}$  of the sample.

To put the measured  $T_{melt}$  of slag #1 and #2 into perspective, the  $T_{melt}$  of an industrial HMD slag sample and of a synthetic HMD slag sample (master slag 2.1) from a previous study [15], are added for comparison. All four samples were analysed with the same equipment and procedure (Table 4).

As expected, based on the theory, the slag with the highest MgO concentration (slag #1) has the highest  $T_{melt}$ . It is observed that slag 2.1, with a similar MgO and Al<sub>2</sub>O<sub>3</sub> concentration as slag #1, has a lower  $T_{melt}$  than slag #1. This is because slag 2.1 contains less CaS (which increases  $T_{melt}$ ) and also contains 0.10 wt-% B<sub>2</sub>O<sub>3</sub>, which lowers  $T_{melt}$ . The much lower  $T_{melt}$  of the industrial HMD slag sample is caused by the high FeO<sub>x</sub> concentration. According to literature, an increase from 0 wt-% to 20 wt-% of FeO<sub>x</sub> in typical BF carryover slag can lower  $T_{melt}$  by 150°C [12].

The melting point measurements show that slag #2, which has an optimal CaO-SiO<sub>2</sub>-Al<sub>2</sub>O<sub>3</sub>-MgO distribution for HMD

slag according to the theory from part I, has a lower  $T_{melt}$  than a synthetic HMD slag. However, when comparing slag #2 with (synthetic) slags with an added slag modifier (containing fluorides or alkali oxides), a lower  $T_{melt}$  can be achieved. Under industrial conditions, the  $T_{melt}$  of a slag with the same relative CaO, SiO<sub>2</sub>, Al<sub>2</sub>O<sub>3</sub> and MgO concentration as slag #2 will be lower than 1416°C, as a result of FeO<sub>x</sub> and other minor oxides. This is illustrated by the comparison of the industrial HMD slag and synthetic slag 2.1.

It should be noted that industrial HMD slag does not have a specific  $T_{melt}$ , but rather a melting temperature trajectory. However, for understanding of the correlations between temperature, slag composition, viscosity and iron losses, a single  $T_{melt}$  is sufficient.

### Apparent viscosity

A Bahr VIS-403 HF rotational viscometer was used to measure the viscosity of the synthetic slags continuously under inert conditions. This machine measures the torque applied to a constant speed rotating bob submerged in a known volume of slag. The viscosity is calculated by the ratio of shear stress ( $\tau$ , in Pa) to shear rate ( $\dot{\gamma}$ , in s<sup>-1</sup>). For a Newtonian fluid contained within two concentric cylinders (Taylor-Couette flow), the shear rate is set according to Equation (7) and the resulting shear stress is measured by Equation (8):

$$\dot{\gamma} = \omega_s \cdot \frac{2R_c^2}{R_c^2 - R_s^2} \quad (7)$$

$$\tau = \frac{Tor}{2\pi \cdot R_s^2 \cdot h_s} \quad (8)$$

where  $\omega_s$  is the rotational speed of the spindle (rad s<sup>-1</sup>),  $R_c$  and  $R_s$  are the radius of the crucible and the spindle respectively (m),  $Tor$  is the measured torque (N·m) and  $h_s$  is the height of the spindle head (m).

Torque measurements were calibrated at room temperature using three certified silicon oils between 0.1 and 1.0 Pa·s. Regression analysis was used to determine the calibration curve. The calibration was specific to the rotation speed selected for the tests. A temperature calibration was determined by measuring the sample temperature at various steps up to 1600°C. The sample temperatures were measured with an R-type thermocouple fed into the crucible inside the viscometer furnace. Regression analysis was applied to the slag temperature measurements in conjunction with the furnace temperature measurements to determine the calibration curve.

For every test, 24 g of prefused powdered slag was put into the crucible and inserted into the rotational viscometer. The oxygen level in the furnace chamber was lowered with an argon purge at 200 ml min<sup>-1</sup>, to protect the molybdenum crucible and spindle from oxidation. The sample was heated to 1600°C whereby the rotating spindle was submerged into the liquid sample. A constant rotation speed of

**Table 3.** X-ray fluorescence (XRF) analysis of synthetic slags #1 and #2 for viscosity and melting range measurements. For comparison, composition of an industrial HMD slag (HMD) and of another synthetic slag, both from a previous study [15], are added. Compositions are in wt-%.

	CaO	SiO <sub>2</sub>	Al <sub>2</sub> O <sub>3</sub>	MgO	Na <sub>2</sub> O	CaS	Fe <sub>2</sub> O <sub>3</sub>	P <sub>2</sub> O <sub>5</sub>	TiO <sub>2</sub>	Cr <sub>2</sub> O <sub>3</sub>
<b>Slag #1</b>	38.83	29.98	10.66	15.80	0.27	4.06	0.24	0.05	0.05	0.05
<b>Slag #2</b>	40.47	29.54	15.27	10.55	0.73	3.10	0.18	0.07	0.05	0.04
<b>HMD</b>	34.24	17.30	6.33	10.06	0.21	4.51	24.26	0.12	0.84	–
<b>Slag 2.1</b>	43.63	26.79	9.81	14.80	0.19	2.83	0.32	–	–	–

**Table 4.** Measured  $T_{melt}$  for Slag #1 and #2, compared with an industrial and synthetic HMD slag.

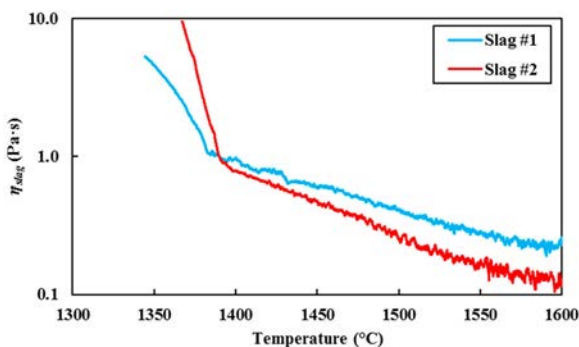
Sample	$T_{melt}$ (°C)
Slag #1	1438
Slag #2	1416
Industrial HMD slag [15]	1334
Synthetic HMD slag 2.1 [15]	1424

280 rev min<sup>-1</sup> was used for the test. The sample was cooled at 10°C min<sup>-1</sup> until the sample reached a maximum torque of 25 mNm.

Figure 10 shows that both slags have a low  $\eta_{slag}$  (<1 Pa·s) at temperatures >1390°C. At these temperatures, MgO and Al<sub>2</sub>O<sub>3</sub> have an effect on  $\eta_{slag}$ : a lower MgO concentration leads to a lower  $\eta_{slag}$ . However, at  $\eta_{slag}$  < 1 Pa·s, its effect on iron losses in industry will be negligible. At some point below 1390°C, there is a marked increase in the viscosity of both slags. This is due to the growth of solid particles causing a dramatic resistance to liquid flow. Below 1390°C,  $\eta_{slag}$  is higher for slag #2 (with less MgO) than for slag #1, while based on theory it was expected that MgO leads to a higher solid fraction. Furthermore, the viscosity measurement suggests that slag #1 has a lower solidification temperature than slag #2, while the melting temperature experiments show that slag #2 has the lowest  $T_{melt}$ . A possible explanation for this is that when the slag is cooled down from 1600°C during the experiment, the cooling goes faster than in industrial practice, producing a super-cooled liquid, so the slag is not at equilibrium, which leads to the formation of MgAl<sub>2</sub>O<sub>4</sub>-rich spinel, melilite, CaS, Ca-Mg-orthosilicate (Ca<sub>3</sub>MgSi<sub>2</sub>O<sub>8</sub>) compound formation at low temperature which increases  $\eta_{slag}$ . Due to the cooling rate of 10°C min<sup>-1</sup> and the composition of slag #1, it is possible that more super-cooled liquids were present [16].

To validate if the quick cooling of the slag during the experiment caused the higher viscosity, the viscosity of slag #1 and #2 at the temperature range of 1370–1600°C are modelled with FactSage 7.3 [2]. Here  $\eta_{slag}$  is determined via the Einstein-Roscoe equation (Equation (5)). Figure 11 shows the experimental  $\eta_{slag}$  versus the thermodynamic  $\eta_{slag}$  under the same conditions.

The comparison shows that at  $\eta_{slag}$  < 0.7 Pa·s, the experiments give a greater  $\eta_{slag}$  than the equilibrium calculations. When comparing slag #1 and #2, at  $\eta_{slag}$  > 2 Pa·s, experiments give a lower  $\eta_{slag}$  for slag #1, while the experiments almost always predict a higher  $\eta_{slag}$  than the equilibrium calculations for slag #2. The equilibrium calculations in FactSage show the formation of the  $\eta_{slag}$ -increasing solids.

**Figure 10.** Viscosity measurements for slag #1 and #2 at different temperatures.

Under industrial HMD conditions, the temperature of the slag changes very slowly (typically the temperature decreases with 0.5°C min<sup>-1</sup>). Therefore, it is likely that the slag conditions are closer to the equilibrium situation than to the fast cooling experimental conditions. This means that the experiments overestimate  $\eta_{slag}$  at temperatures below 1390°C for slag #2 when compared to the industrial HMD process. Note that, despite the small changes in temperature, the industrial HMD slag is constantly changing composition during the process, so it is not necessarily at equilibrium.

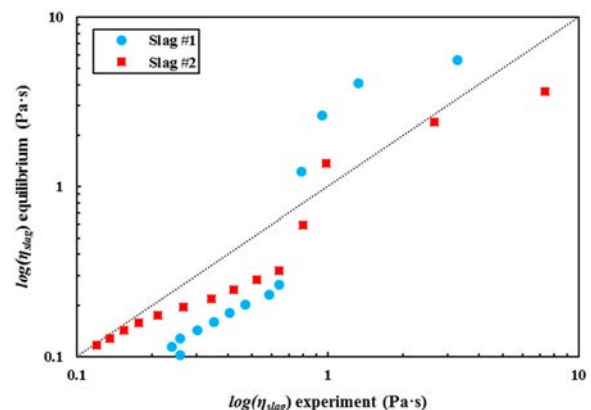
## Discussion

### Validation

In part I of this study [1], claims were made about the composition of the optimal HMD slag, regarding sulphur removal capacity and iron losses, based on a theoretical study. In the current part II, these claims are put to the test with a thermodynamic MCS study, industrial plant data analysis and laboratory experiments with synthetic HMD slag.

The sulphur removal capacity, in the thermodynamic MCS study represented with the  $C_s$ , indeed depends on the CaO concentration of the slag. It is noteworthy that, although the injected Mg mostly determines the desulphurisation, the final form of Mg, MgO, does not contribute to the  $C_s$  of the slag. The claim that the  $B2 > 1.1$  is required for the HMD process could not be validated with the plant data, as no heats were found were  $B2 < 1.3$ . The penalty for having a too low sulphur removal capacity is much higher than the penalty for increased iron losses as a result of a higher  $B2$ . So, since iron losses are more or less constant for  $B2 < 1.7$ , it is not strange that no heats were found with a too low  $B2$ ; the steel plant will always try to be on the safe side.

With respect to the iron losses, the trends predicted by the theory regarding the influence of the different components in the slag on the iron losses, are confirmed by the thermodynamic MCS study, the plant data and the laboratory experiments. However, the importance of this influence seems to be different. Based on the theory and the thermodynamics, the MgO concentration of the slag should be as low as possible and preferably MgO < 10 wt-%. However, the plant data show no significant influence of MgO on the iron losses for MgO < 14 wt-%. The reason for this is the slag's temperature. As MgO lowers  $T_{melt}$  of the slag, it will only significantly

**Figure 11.** Measured viscosity versus equilibrium viscosity at the same temperature (range: 1370–1600°C), according to FactSage for slag #1 and #2 on a logarithmic scale.

influence the iron losses if it brings  $T_{melt}$  below the temperature of the slag. This is confirmed by the melting point and viscosity experiments, where MgO hardly influences  $\eta_{slag}$  above  $T_{melt}$ . This means that it depends on the slag and hot metal temperatures at a specific HMD station which MgO concentration in the slag is still acceptable. It should be noted that the temperatures at the HMD stations of Tata Steel IJmuiden are relatively high compared to most other steel plants. Therefore, in most other plants the maximum allowed MgO will be lower than 14 wt-%.

The influence of CaO on the iron losses is comparable to that of the influence of MgO, as CaO also increases  $\eta_{slag}$  and thus the iron losses, mostly by increasing  $T_{melt}$ . Plant data show that higher CaO concentrations (or  $B2$  values) are more acceptable than expected based on the theory and thermodynamics. In practice, for  $B2 > 1.1$  iron losses do not immediately increase. Only when the  $B2$  reaches a certain threshold, 1.7 for the given plant conditions, a further increase in  $B2$  will lead to higher iron losses. As with MgO, the maximum allowed  $B2$  depends particularly on the slag temperature. Higher slag temperatures mean higher  $B2$  values can be reached without increasing the iron losses.

In this part of the study, there is less focus on the influence of the other slag elements on the iron losses. The thermodynamic MCS study gives comparable results as the theory. According to the MCS,  $\text{Na}_2\text{O}$  and  $\text{K}_2\text{O}$  have a relatively large impact on  $T_{melt}$ , despite their low concentrations. This explains why these alkali metal oxides are suited as slag modifiers, as they lower  $\eta_0$  [15].

The melting range experiments showed that  $\text{FeO}_x$  significantly lowers  $T_{melt}$ . This confirmed the FactSage calculations about the addition of FeO to the slag from part I. In the MCS the influence of FeO on  $X_{solid}$  was small, because the MCS was done under inert conditions, with a wide range of temperatures, which meant the influence of FeO on  $T_{melt}$  had only a small effect on  $X_{solid}$ . However, under industrial conditions,  $\text{FeO}_x$  will lower  $X_{solid}$  and, thus, the iron losses.

### Industrial implications

Based on the theory, explained in part I of this study, and plant trials at the former Tata Steel plant in Scunthorpe, UK, around 2010 [6], the minimal  $B2$  of the slag for sufficient sulphur removal is 1.1. Besides, enough magnesium should be injected to remove the sulphur. Stoichiometrically a Mg:S weight ratio of 0.76:1 is sufficient, but due to Mg dissolution in hot metal and kinetic constraints, a minimal Mg:S weight ratio of 1:1 is required. However, in most steel plants typically more Mg and CaO are injected than necessary, to be on the safe side, as the penalty for not achieving the final sulphur aim is supposed to be higher than the costs of extra reagents. The resulting increased iron losses are usually not monitored accurately, so their costs are often overlooked. Therefore, in general HMD slags typically have higher CaO and MgO concentrations than necessary, which increases the slag's  $T_{melt}$ .

Although the slag's viscosity, its solid fraction and the size and shape of solids all influence the colloidal iron losses during the HMD process, in practice the solid fraction, which heavily influences  $\eta_{slag}$ , determines these colloidal iron losses. This means that, in order to keep the iron losses as low as possible, the slag should have a low  $T_{melt}$ . Under industrial HMD conditions this means CaO and MgO concentrations should be kept as low as possible. Steel plants where the hot

metal (and slag) temperatures are typically high will have more freedom to inject extra CaO and Mg than steel plants where the hot metal temperatures are typically lower, as high slag temperatures allow for a higher  $T_{melt}$ . This also means that if a change in the BF process or the hot metal transport time lead to lower temperatures, adjustments in the HMD process might be required to avoid an increase in iron losses.

At the HMD, the temperature of the slag is difficult to increase. In general, steel plants already try to keep the temperature of the hot metal (and slag) as high as possible. However, other adjustments, to lower the iron losses are more practical:

- At the BF, the MgO concentration in the carryover slag can be decreased, to lower  $T_{melt}$ . Decreasing the total amount of carryover slag would be beneficial as well, but this is in practice harder to achieve.
- During the HMD process, the amount of injected CaO and Mg can be lowered, if the desulphurisation requirements allow. This decreases  $T_{melt}$  and also slightly lowers the total slag amount.
- Slag modifiers, which lower  $T_{melt}$  and/or  $\eta_{slag}$ , like  $\text{Na}_2\text{O}$  and  $\text{K}_2\text{O}$ , can be added.
- Increase the time between reagent injection and slag skimming, to give entrapped iron more time to drip back into the metal bath. However, this increases the process time, which could lead to a lower productivity if the HMD is the bottleneck in the steel plant.

### Conclusions

The validation of the fundamentals of the optimal HMD slag, considering sulphur removal capacity and iron losses, using a thermodynamic MCS, a plant data analysis and viscosity and melting point measurements in a laboratory, confirmed the initial conclusions. However, some additional remarks can be made based on this study:

- To achieve the desired sulphur removal capacity, the slag should contain at least enough CaO to allow all MgS to react with CaO to form CaS. Besides, a minimal CaO:SiO<sub>2</sub> weight ratio ( $B2$ ) in the slag of 1.1 is required.
- A lower CaO and MgO concentration in the slag does lead to a lower  $\eta_{slag}$  and thus to lower iron losses, but as soon as  $T_{melt}$  of the slag is lower than the slag temperature, the optimal CaO and MgO concentration is reached. A further decrease in CaO would be even unwanted as it would lower the sulphur removal capacity of the slag.
- The slag weight contributes much less to the iron losses than  $\eta_{slag}$ .

### List of symbols and abbreviations

#### Symbols

$a_O$	Oxygen activity (-)
$B2$	Basicity CaO/SiO <sub>2</sub> (-)
$C_S$	Sulphide capacity (-)
$h_x$	Height of x (m)
$n$	Constant (Equation (4); typically 2.5) (-)
$p_x$	Partial pressure of x (Pa)
$R_x$	Radius of x (m)
$T$	Temperature (°C)
$T_{melt}$	Melting temperature (°C)
$Tor$	Measured torque (N·m)

$X_{(S)}$	Sulphide weight percentage in the slag (wt-%)
$X_x$	Weight fraction of x (component or phase) (wt-%)
$\alpha$	Maximum solid fraction (Equation (4)) (-)
$\dot{\gamma}$	Shear rate ( $s^{-1}$ )
$\eta_0$	Viscosity of the liquid fraction of the slag (Pa·s)
$\eta_{slag}$	Apparent viscosity of the slag (Pa·s)
$\tau$	Ratio of shear stress (Pa)
$\varphi_{s,slag}$	Solid volume fraction of the slag (-)
$\omega_x$	Rotational speed of x ( $rad\ s^{-1}$ )

## Disclosure statement

No potential conflict of interest was reported by the author(s).

## ORCID

Frank N. H. Schrama  <http://orcid.org/0000-0001-9172-4175>

Elisabeth M. Beunder  <http://orcid.org/0000-0001-8734-9261>

Adam Hunt  <http://orcid.org/0000-0002-5423-6313>

Jilt Sietsma  <http://orcid.org/0000-0001-8733-4713>

Rob Boom  <http://orcid.org/0000-0002-0519-0208>

Yongxiang Yang  <http://orcid.org/0000-0003-4584-6918>

## References

- [1] Schrama FNH, Beunder EM, Panda SK. Optimal hot metal desulphurisation slag considering iron loss and sulphur removal capacity I: Fundamentals. *Ironmak Steelmak*. 2021, doi:10.1080/03019233.2021.1882647.
- [2] CRCT (Canada) & GTT (Germany), "FactSage 7.3," 2020. [Online]. [www.factsage.com](http://www.factsage.com).
- [3] Schrama FNH, Beunder EM, van den Berg B, et al. Sulphur removal in ironmaking and oxygen steelmaking. *Ironmak Steelmak*. 2017;44(5):333–343. doi:10.1080/03019233.2017.1303914.
- [4] Visser H-J. Modelling of injection processes in ladle metallurgy [PhD thesis]. Delft University of Technology, Delft (NL); 2016.
- [5] Kitamura S. Hot metal pretreatment. In: S Seetharaman, editor. *Treatise on process metallurgy*, vol. 3. Oxford: Elsevier; 2014. p. 177–221.
- [6] Li Z, van Boggelen JWK, Thomson H, et al. Improved slag skimming performance at hot metal desulphurisation station by using recycled materials as slag modifying agent. in *Scanmet IV*, 2012, p. 189–195.
- [7] Roscoe R. The viscosity of suspension of rigid spheres. *Br J Appl Phys*. 1952;3(Aug):267–269.
- [8] Li Z, Bugdol M, Crama W. Optimisation of hot metal desulphurisation slag in the CaO / Mg co-injection process to improve slag skimming performance. in *Molten2012*. 2012.
- [9] Moosavi-Khoonsari E, Jung IH. Thermodynamic modeling of sulfide capacity of Na<sub>2</sub>O-containing oxide melts. *Metall Mater Trans B*. 2016;47(5):2875–2888. doi:10.1007/s11663-016-0749-z.
- [10] Panda SK, Harbers E, Overbosch A, et al. Desulphurization with ladle furnace slag. In *Proceedings of METEC & 4th ESTAD*, 2019; P264.
- [11] Chatterjee S, Konar B, Maity A, et al. Development of alternative flux for liquid steel desulfurization. In *AISTech 2019 — Proceedings of the Iron & Steel Technology Conference*, 2019, p. 1211–1224. <https://doi.org/10.33313/377/123>.
- [12] Geerdes M, Chaigneau R, Kurunov I, et al. *Modern blast furnace Ironmaking*. 3rd ed. Delft (NL): IOS Press; 2015.
- [13] Yang Y, Raipala K, Holappa L. Ironmaking. In: S Seetharaman, editor. *Treatise on process metallurgy*, vol. 3. Oxford (UK): Elsevier; 2014. p. 2–88.
- [14] Street S, Stone RP, Koros PJ. The presence of titanium in hot metal and its effects on desulfurization. *Iron Steel Technol*. 2005;2(11):65–74.
- [15] Schrama FNH, Ji F, Hunt A, et al. Lowering iron losses during slag removal in hot metal desulphurisation without using fluoride. *Ironmak Steelmak*. 2020;47(5):464–472. doi:10.1080/03019233.2020.1747778.
- [16] Sun Y, Zhang Z, Liu L, et al. Multi-Stage control of waste heat recovery from high temperature slags based on time temperature transformation curves. *Energies*. 2014;7(3):1673–1684. doi:10.3390/en7031673.